J. Membrane Biol. 146, 91–99 (1995)

The Journal of
Membrane
Biology

Ca^{2+} Modulation of Sarcoplasmic Reticulum Ca^{2+} Release in Rat Skeletal Muscle Fibers

O. Delbono

Departments of Physiology and Pharmacology and Internal Medicine, Section on Internal Medicine and Gerontology, Bowman Gray School of Medicine, Wake Forest University, Winston-Salem, N.C. 27157

Received: 29 June 1994/Revised: 7 March 1995

Abstract. Ca^{2+} transients and the rate of Ca^{2+} release (dCa_{REL}/dt) from the sarcoplasmic reticulum (SR) in voltage-clamped, fast-twitch skeletal muscle fibers from the rat were studied with the double Vaseline gap technique and using mag-fura-2 and fura-2 as Ca^{2+} indicators. Single pulse experiments with different returning potentials showed that Ca^{2+} removal from the myoplasm is voltage independent. Thus, the myoplasmic Ca^{2+} removal (dCa_{REM}/dt) was studied by fitting the decaying phase of the Ca^{2+} transient (Melzer, Ríos & Schneider, 1986) and dCa_{REL}/dt was calculated as the difference between dCa/dt and dCa_{REM}/dt. The fast Ca^{2+} release decayed as a consequence of Ca^{2+} inactivation of Ca^{2+} release. Double pulse experiments showed inactivation of the fast Ca^{2+} release depending on the prepulse duration. At constant interpulse interval, long prepulses (200 msec) induced greater inactivation of the fast Ca^{2+} release than shorter depolarizations (20 msec). The correlation (r) between the myoplasmic $[Ca^{2+}]_i$ and the inhibited amount of Ca^{2+} release was 0.98. The $[Ca^{2+}]_i$ for 50% inactivation of dCa_{REL}/dt was 0.25 μM, and the minimum number of sites occupied by Ca^{2+} to inactivate the Ca^{2+} release channel was 3.0. These data support Ca^{2+} binding and inactivation of SR Ca^{2+} release.

Key words: Ca^{2+} transients — Excitation-contraction coupling — Mammalian skeletal muscle — Mag-Fura-2 — Fura-2 — Ca^{2+} release

Introduction

The depolarization of the skeletal muscle T-tubule membrane is sensed by dihydropyridine-sensitive calcium channels (DHPR) giving rise to gating and ionic currents. DHPRs interact with ryanodine receptors (RYR) (sarcoplasmic reticulum calcium release channel), eliciting calcium release from the sarcoplasmic reticulum. Transient increases in myoplasmic calcium concentration give rise to muscle contraction and relaxation. Voltage- and calcium-gated mechanisms contribute to sarcoplasmic reticulum calcium release. These two mechanisms are mediated by direct DHP-RYR interaction and by calcium, respectively (Jacquemond et al., 1991).

The study of intracellular Ca^{2+} transients with fluorescent indicators revealed basic mechanisms of the excitation-calcium release-contraction signaling pathway in amphibian fibers. Differences in RYR isoforms expression in amphibian and mammalian skeletal muscles stresses the importance of studies on mammals. However, these studies have started more recently (Delbono & Stefani, 1993*b*; García & Schneider, 1993).

Calcium transients in rat fast-twitch fibers show a complex rising phase (Delbono et al., 1993*b*). This observation is less consistent in frog fibers in which simple or complex rising phases, have been described (Kovacs, Ríos & Schneider, 1983; Brum, Ríos & Stefani, 1988). The Ca^{2+} release functions also differs in frog and rat fibers (Melzer, Ríos & Schneider, 1986, 1987; Schneider, Simon & Szücs, 1987; Delbono et al., 1993*b*; García & Schneider, 1993). This might suggest differences in the regulation of Ca^{2+} release by Ca^{2+} and Mg^{2+} (Meissner et al., 1986; Jacquemond et al., 1991; Simon et al., 1991; Delbono & Stefani, 1993*b*). The calcium-dependent inactivation of calcium release in amphibian fibers and in vitro systems have been reported (Baylor et al., 1983; Simon et al., 1988, 1991; O'Brien et al., 1995). However, very little is known about the regulation by calcium of the SR calcium release in living mammalian fibers. In this work, the role of myoplasmic Ca^{2+} on the regulation of SR Ca^{2+} release in rat fast-twitch muscle fibers, have been studied. The high- and low-affinity calcium indicators, mag-fura-2 (Raju, 1989; Konishi et al., 1991) and fura-2, have been used to monitor large and small myoplasmic calcium concentration changes,

Correspondence to: O. Delbono

respectively. These studies allowed the calculation of the calcium concentration needed for half calcium release inactivation and the minimum number of sites occupied by Ca^{2+} to inactivate the channel. Part of this work has been presented elsewhere (Delbono & Stefani, 1993*a*).

Materials and Methods

Fiber Preparation

Single fibers from extensor digitorum longus (EDL) muscle of the rat were manually dissected and mounted according to previous procedures (Delbono et al., 1991; Delbono, 1992). The EDL muscle was dissected after sacrificing the rat in a carbon dioxide chamber. The muscles were kept for 8 to 9 hr in a beaker containing a modified Krebs solution at 4°C. For calcium transient studies, fibers dissected within the first 3 hr after sacrificing the rat were included in this study. Fibers were stretched to 3.6–3.8 μm sarcomere length.

Solutions

The external solution contained (mM): 150 TEA (tetraethylammonium)-$MeSO_3$ (methanesulphonic acid), 2 $CaCl_2$, 2 $MgCl_2$, 2 TEA-HEPES (N-[2-hydroxyethyl]piperazine-N′-[2-ethanesulfonic acid]) and 0.001 TTX (tetrodotoxin), 1 9-anthracenecarboxylic acid, and 1 3-4 diaminopyridine (pH adjusted to 7.2 with TEAOH). The internal solution contained (mM): 98 K-glutamate; 0.1 K_2-EGTA; 0.0082 $CaCl_2$; 5 Na_2ATP; 5.5 $MgCl_2$; 5 glucose; 5 K-HEPES; 5 Na_2-phosphocreatine; pH = 7.2. The osmolarity of the solutions was 300 mosm. Mag-Fura-2 and fura-2 (Molecular Probes, Eugene, OR) were added from 5 mM stock solutions (in deionized water) to final concentrations of 400 μM and 50 respectively. Free Ca^{2+} concentration in solutions were calculated using dissociations constants of ligands from the literature (Fabiato, 1988).

Set-up, Stimulation, Recording and Data Analysis. In vitro and in vivo Calibration

Fibers were voltage-clamped using the double Vaseline gap technique similar to the one introduced by Kovacs, Ríos & Schneider (1983) and modified by Francini and Stefani (1989). The holding potential was −80 mV. Temperature was constantly monitored with a thermistor probe positioned close to the fiber in the middle pool. Hardware included an IBM-compatible AT personal computer with a D-A and A-D conversion, 12 bits, an Axolab-1 computer interface (Axon Instruments, Foster City, CA). Stimulation protocols are detailed in Results for each group of experiments. Fluorescent signals were filtered at 0.3 of the sampling frequency (−3 Db point) with a 4-pole Butterworth low-pass filter (Frequency Devices, Haverhill, MA). Background autofluorescence was recorded before the addition of the dye to both end pools and was subtracted from all optical records. Fluorescence signals were normalized to the basal dye fluorescence of the fiber in resting conditions (without stimulation) or converted into Ca^{2+} concentration. All the experiments were carried out at 17 ± 0.2°C. Values are given as means ± SEM with n as the number of observations.

Calibrations of mag-fura-2 were performed in a double-beam spectrofluorometer (SLM Aminco Instruments, Urbana, IL) in cuvettes. Calibrations were also performed in the recording set-up using thin glass capillary cells (Vitro Dynamics; 0.1 mm path length and 2 mm width). The range of excitation wavelength in the spectrofluorometer was 300–450 nm. In the recording setup using the optical path used for Ca^{2+} transients recordings excitation wavelength were 350 (isosbestic point) and 380 nm. Solutions with different Ca^{2+} concentrations were prepared following Tsien & Pozzan (1989).

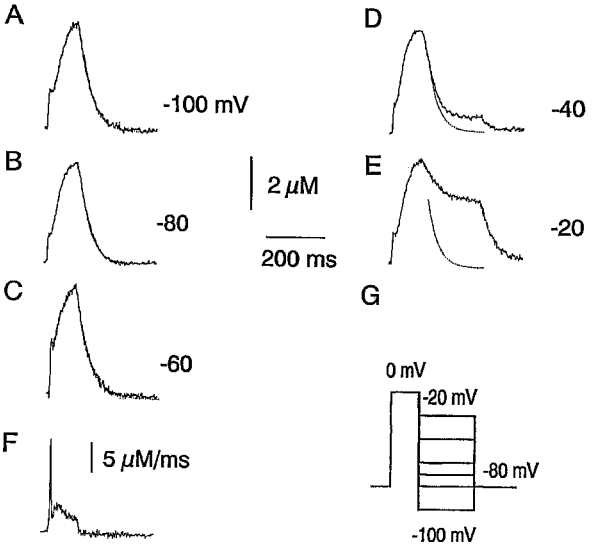

Fig. 1. Voltage-independence of myoplasmic Ca^{2+} removal. Ca^{2+} transients were recorded with mag-fura-2 (*A–E*) with pulses from V_h-80 mV to 0 mV and varying the potential after the test pulse from −100 to −20 mV (*G*). The Ca^{2+} transients decaying phases were fitted to a single exponential function and superimposed as dotted lines to each trace. Calculated Ca^{2+} release for the traces in *A, B* and *C* is illustrated in *F*. The fitting to traces *A* to *C* was superimposed to the records in *D* and *E,* as dotted lines.

Calculation of Ca^{2+} Release

To obtain the rate of Ca^{2+} release (dCa_{REL}/dt), the model proposed by Melzer et al. (1986), Melzer, Ríos & Schneider (1987) and the mathematical formulations (Appendix) by Brum, Ríos & Schneider in Brum, Ríos & Stefani (1988), was used. This method gave the rate of Ca^{2+} release from [dCa^{2+}/dt] = input flux-output flux. The input flux corresponds to the rate of Ca^{2+} release, while the output flux to the rate of Ca^{2+} removal (dCa_{REM}/dt). No correction for SR Ca^{2+} depletion was applied. A set of parameters was obtained by fitting calcium traces of different duration and amplitude (González & Ríos, 1993). This set of values was applied to the double pulse experiments.

Voltage-independence of the Rate of Removal of Myoplasmic Ca^{2+}

Since the calculation of the rate of Ca^{2+} release is based on the assumption that the rate of Ca^{2+} removal is voltage independent, we studied the effect of different returning potentials on the decaying phase of the Ca^{2+} transient. Figure 1 shows Ca^{2+} transients recorded with mag-fura-2 using pulses from V_h-80 mV to 0 mV and different returning potentials from −100 to −20 mV (pulse protocol in *G*). The Ca^{2+} transient decaying phases after pulses to 0 mV were fitted to a single exponential function and superimposed as dotted line to each trace. The decay time constants were not altered by postpulses to −100

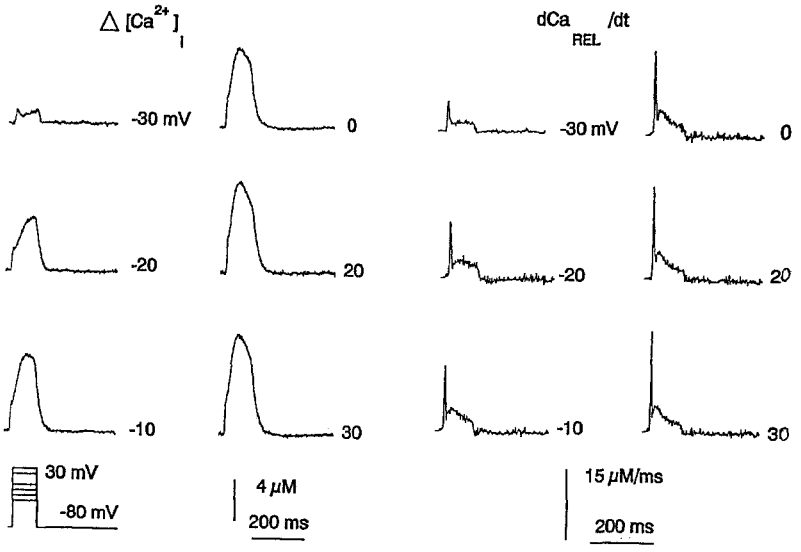

Fig. 2. Voltage-dependence of Ca^{2+} release inactivation. Ca^{2+} transients ($\Delta[Ca^{2+}]_i$) monitored with mag-fura-2, at potentials from −30 to 30 mV (pulse protocol at the bottom) and the corresponding calculated SR Ca^{2+} release (dCa_{REL}/dt) are shown on the left and on the right, respectively. The calculated Ca^{2+} release decays monotonically after an initial peak. The Ca^{2+} release decaying phase was fitted from the peak to the inflection where a change of the slope is recorded.

mV, −80 and −60. Their values were 30.6 ± 1.2, 29.7 ± 1.1 and 30.3 ± 1.7, respectively (n = 5; $P > 0.05$). As expected, for larger returning potentials (−40 mV and −20 mV), the decay phase had a slower time constant since those potentials induced Ca^{2+} release. The dotted lines in *D* and *E* correspond to the fitted decay phase in *A*. The calculated Ca^{2+} release for the traces in *A*, *B* and *C* are represented in *F*.

In summary, Ca^{2+} transients decayed independently of the repolarizing potential (−100 mV to −60 mV). Thus, double pulses were used in this work to study changes in SR Ca^{2+} release induced by myoplasmic Ca^{2+}.

Results

Voltage-independence of the Initial Peak Ca^{2+} Release Inactivation

Figure 2 shows Ca^{2+} transients and the rate of Ca^{2+} release function (dCa_{REL}/dt) detected with mag-fura-2 at different potentials (−30 to +30 mV). Ca^{2+} transients were larger and faster with depolarization. The amplitude saturated at about +20 mV. At −30 mV, the initial and second components of the Ca^{2+} transient had similar amplitudes. The corresponding rate of Ca^{2+} release shows a peak that rapidly inactivates followed by a steady state phase or plateau. For larger depolarizations (−20 to +30 mV), a second rising phase appeared in the Ca^{2+} transients, after the initial peak of Ca^{2+} release. During the pulse, this second Ca^{2+} release component showed a slow decay which was more pronounced at more positive potentials. This slow decay during the pulse has been attributed to sarcoplasmic reticulum (SR) Ca^{2+} depletion in frog fibers.

A single exponential function was fitted to the decaying phase of the peak Ca^{2+} release. The Ca^{2+} release inactivation time constants were not modified by the pulse amplitude. The values were (msec): 18.1 ± 2.3, 17.7 ± 3.1, 21.7 ± 2.7, 20.0 ± 2.5, 23.1 ± 2.9 and 20.0 ± 2.3 at −30, −20, −10, 0, +20 and +30 mV, respectively (n = 12; $P > 0.05$). These data indicate that depletion of the SR Ca^{2+} is not a major cause for the interruption of the fast peak of Ca^{2+} release. Similar conclusions were reported for frog skeletal muscle fibers (Simon & Schneider, 1988). If SR Ca^{2+} depletion were involved in the peak Ca^{2+} release falling phase, its time constant would have been faster at more positive potentials when larger amounts of Ca^{2+} are released. In summary, these data support the concept that Ca^{2+} release channel inactivation is the major cause for the abrupt decline in Ca^{2+} release few milliseconds after depolarization.

Influence of Prepulse and Interpulse Duration on the Amplitude of Ca^{2+} Release

Figures 3 to 5 show that the peak Ca^{2+} release was reduced (inactivated) when a test pulse was preceded by a prepulse. To study the time course of recovery from inactivation, different double-pulse protocols were applied. To eliminate possible effects of resting Ca^{2+} concentration on prepulse, stimulation protocols were applied at various intervals. When the double pulses were repeated every 2.5 minutes, the basal Ca^{2+} concentration at the beginning of each sweep remained practically unmodified (*see* Fig. 7, dotted lines), and Ca^{2+} transients in response to prepulses, were reproductive.

Figure 3 shows Ca^{2+} transients (*A*) and their corresponding calculated rate of Ca^{2+} release dCa_{REL}/dt (*B*) with the pulse protocol illustrated in *C*. Constant pre- and test-pulses (30 msec and 50 msec, respectively), and variable interpulses (30 to 700 msec), were used. Last records in *A* and *B* were obtained by summation of pre- and test-pulses (80 msec). Ca^{2+} transients were larger in

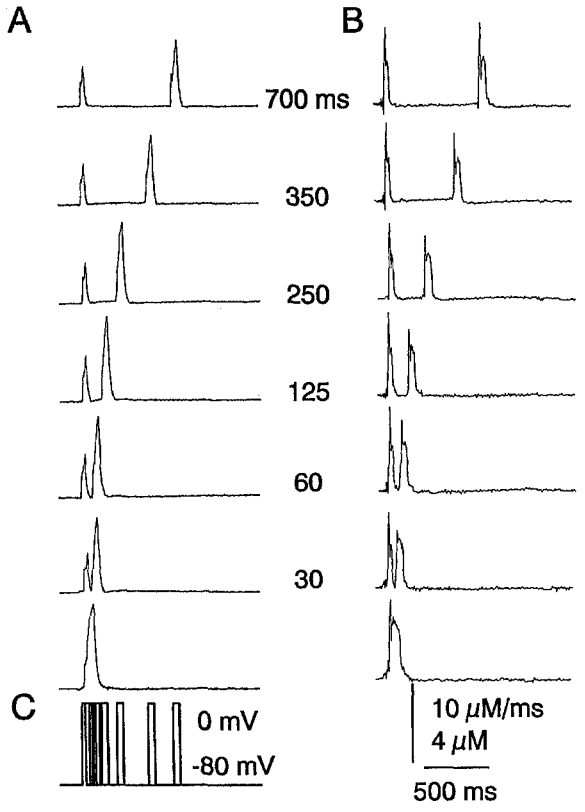

Fig. 3. Recovery from inactivation of Ca^{2+} release with 30 msec-prepulses. (*A*) Ca^{2+} transients monitored with mag-fura-2 and elicited with double pulse protocols. (*B*) Calculated SR Ca^{2+} release corresponding to the traces in *A*. The interpulse duration is shown between traces. The last two traces correspond to Ca^{2+} transient and their calculated Ca^{2+} release obtained with 80 msec-pulse duration. (*C*) Pulse protocol.

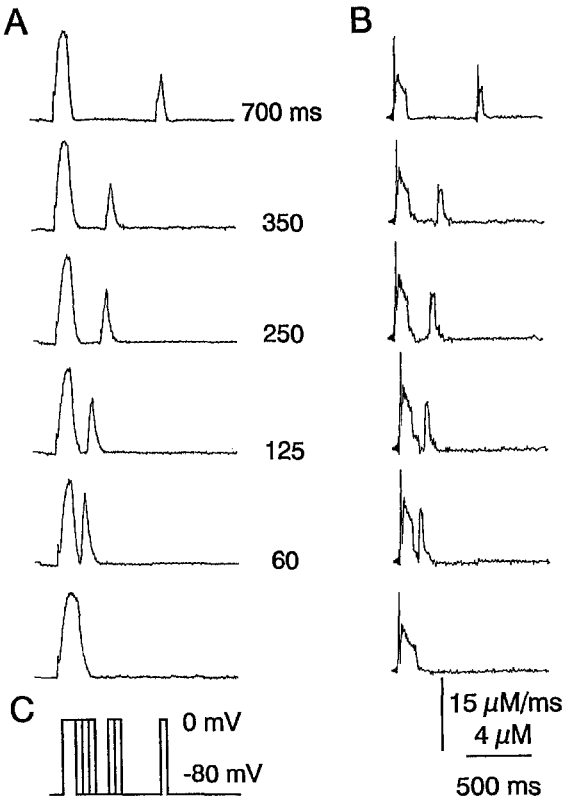

Fig. 4. Recovery from Ca^{2+} release inactivation with 120 msec prepulses. (*A*) Ca^{2+} transients monitored with mag-fura-2, were elicited with double pulse protocols. (*B*) Calculated SR Ca^{2+} release corresponding to the traces in *A*. The interpulse duration is shown between traces. The last two traces correspond to Ca^{2+} transient and its calculated Ca^{2+} release obtained with 170 msec-pulse duration. (*C*) Pulse protocol.

response to test pulses than to prepulses due to different pulse durations. As the pulse interval was shortened, Ca^{2+} transients became larger with a slower rising phase and the rate of Ca^{2+} release showed a progressive reduction of the peak amplitude. The slower rising phase together with a smaller rate of Ca^{2+} release may reflect a Ca^{2+}-induced inactivation of the SR Ca^{2+} release.

Figure 4 shows Ca^{2+} transients and the rate of Ca^{2+} release with the same interpulse intervals but with longer prepulse durations (120 msec). When longer prepulses were applied, peak Ca^{2+} release was reduced more markedly for equivalent interpulse durations compared to those used in Fig. 3. The fast component of Ca^{2+} release was undetectable with 125 msec or shorter interpulse intervals. These data suggest that the higher the myoplasmic Ca^{2+} concentration, the more pronounced the SR Ca^{2+} release inactivation.

Figure 5 shows the time course of recovery of the peak Ca^{2+} release during test pulses at different interpulse durations (t), with 30, 60 and 120 msec prepulses (n = 8 for each set of data). Values were normalized as peak release(t)/peak release ($t = \infty$) or (peak test pulse dCa_{REL}/dt)/(peak prepulse dCa_{REL}/dt). The peak Ca^{2+} release inactivation was more pronounced with longer prepulses and shorter intervals. For example, the degree of inactivation for the 125 msec interval pulse were 0.77, 0.68, respectively, and unmeasurable for 30, 60 and 120 msec prepulses. With 30 msec prepulses, the inactivation was less prominent and a complete recovery from inactivation was recorded using 700 msec pulse interval.

After the prepulse, the myoplasmic Ca^{2+} concentration remained high for variable times, although this was not detected because of mag-fura-2 has low affinity for Ca^{2+} (K_D = 49 μM). The amount of the residual myoplasmic Ca^{2+} at the moment of applying the test pulse depends on the prepulse amplitude and duration. The influence of $[Ca^{2+}]$ on SR Ca^{2+} release inactivation was also studied using prepulses with constant duration and variable amplitude.

Effect of Prepulses with Constant Duration and Variable Amplitude on SR Ca^{2+} Release Inactivation

Figure 6 shows Ca^{2+} transients ($\Delta[Ca^{2+}]_i$) and their corresponding rate of Ca^{2+} release by applying long pre-

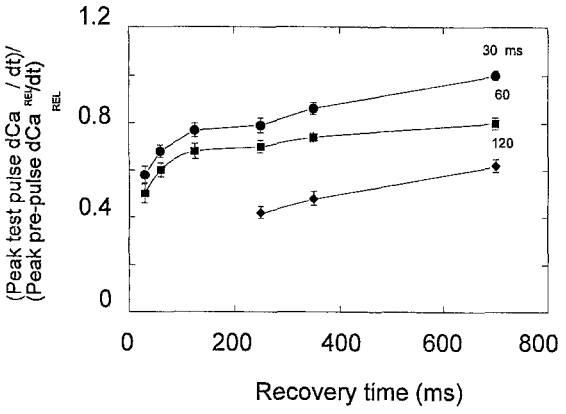

Fig. 5. Influence of the prepulse duration on the recovery time from Ca^{2+} release inactivation. The relationship of (peak test pulse dCa_{REL}/dt)peak prepulse dCa_{REL}/dt)—recovery time, is represented as a function of the prepulse duration (30, 60 and 120 msec). Values are means ± SEM.

pulses (200 msec) at different voltages (−45 to −15) separated by a constant 20 msec interval from the test pulse (0 mV, 200 msec duration). Ca^{2+} transients elicited by the test pulses without prepulse were biphasic, as described above. As the myoplasmic Ca^{2+} concentration increased in response to the prepulse, both Ca^{2+} transient components were not clearly distinguished. Calculated Ca^{2+} release functions showed a fast peak that did not exhibit the time course obtained with more positive pulses. Ca^{2+} release induced by prepulses were detected from −45 to −40 mV. At −30 mV, the fast Ca^{2+} release during the test pulse practically disappeared. At −40 and −35 mV, changes in the time course of the second Ca^{2+} release phase, were detected. In summary, in these experiments, alterations in the rate of Ca^{2+} release depends on the amount of SR Ca^{2+} released in response to the prepulse.

Effect of Resting $[Ca^{2+}]_i$ on SR Ca^{2+} Release Monitored with Fura-2

One of the assumptions made in the previous sections was that $[Ca^{2+}]_i$ does not return immediately to predepolarization concentrations after repolarization. Moreover, the amount of the residual $[Ca^{2+}]_i$ was highly correlated with the amount of Ca^{2+} released in response to prepulses. Figure 7A shows Ca^{2+} transients elicited by the pulse protocol depicted in *B* and monitored with fura-2. A 20 msec pulse from $V_h = -80$ mV to 0 mV saturated almost completely the dye. As the pulse duration was increased from 40 msec to 300 msec higher $[Ca^{2+}]_i$ were detected after fiber repolarization. *C* shows Ca^{2+} transients elicited by the pulse protocol illustrated in *D*. Calcium fluxes corresponding to similar pulses and measured with mag-fura-2 are shown in Figs. 3 to 5.

Ca^{2+} transients elicited by a double pulse protocol were performed to determine the amount of residual $[Ca^{2+}]_i$ at the moment of applying test pulses (Fig. 7*C*). Despite using 3 min interval between sweeps, the resting $[Ca^{2+}]_i$ before the prepulse increased slightly. The zero level is represented by the dotted lines in *C*, and *a* corresponds to the $[Ca^{2+}]_i$ at the end of the prepulse. The residual $[Ca^{2+}]_i$ at the moment of applying the test pulse is labeled as *b*. As the interpulse was shortened, the second pulse was applied at increasing $[Ca^{2+}]_i$. The point *b* is a measurement of the myoplasmic Ca^{2+} concentration immediately before the test pulse and is expressed as a fraction of the Ca^{2+} transient amplitude during the prepulse. Normalized *b* values were: 0.13 ± 0.03, 0.25 ± 0.06, 0.70 ± 0.08, 0.91 ± 0.11 and 0.97 ± 0.14 (n = 9) for 750, 350, 125, 60 and 10 msec interval, respectively.

The influence of the residual $[Ca^{2+}]_i$ on Ca^{2+} release can be better seen by plotting normalized *b* and P_1 (P_1 is defined as the ratio between (peak test pulse dCa_{REL}/dt)/(peak prepulse dCa_{REL}/dt)) values *vs.* the interpulse intervals. The experiments included in this plot correspond to those of 60 msec prepulses. Figure 8*A* shows that, as the interval between pulses was shortened, the residual $[Ca^{2+}]_i$ was increased greatly affecting the peak Ca^{2+} release amplitude. Fig. 8*B* shows the correlation between normalized P_1 and *b* ($r = 0.98$).

The Ca^{2+} dependence of the peak dCa_{REL}/dt inactivation can be examined by plotting the ratio between the peak Ca^{2+} release (P_1), and the maximum release during the second Ca^{2+} release phase (P_2) of the test pulse, at different Ca^{2+} concentrations. Fig. 8*C* is a semilogarithmic plot of (P_1/P_2)-1 *vs.* $[Ca^{2+}]_i$. Ca^{2+} concentrations used in this graph were calculated from fura-2 determinations immediately prior to the test pulse (*b* in Fig. 7). Data from 8 fibers were fitted to the following equation:

$$(P_1/P_2) - 1 = (f_P/K_S)((K_F K_S)/(1 + K_S))/((KF_F K_S)/(1 + K_S)) + [Ca^{2+}]^n);$$

where, according to a model of channel inactivation based on binding of multiple Ca^{2+} (Simon et al., 1991), f_P is a correction factor, K_S and K_F are the dissociation constants for the rapidly and slowly equilibrating steps between the free receptor and the receptor-Ca^{2+} complex, and from this complex to the inactivated state, respectively; and $[Ca^{2+}]^n$ is the Ca^{2+} concentration immediately before the test pulse. The $[Ca^{2+}]_i$ for 50% inactivation of dCa_{REL}/dt and the minimum number of sites that must be occupied by Ca^{2+} to induce inactivation (n) were 0.25 μM and 3, respectively. In summary, these observations suggest that Ca^{2+} release inactivation is highly correlated with residual $[Ca^{2+}]_i$, and a threefold increase in the resting $[Ca^{2+}]_i$ is necessary to induce half inactivation of SR Ca^{2+} release. It seems that at least three sites should be occupied by Ca^{2+} before inactivation occurs.

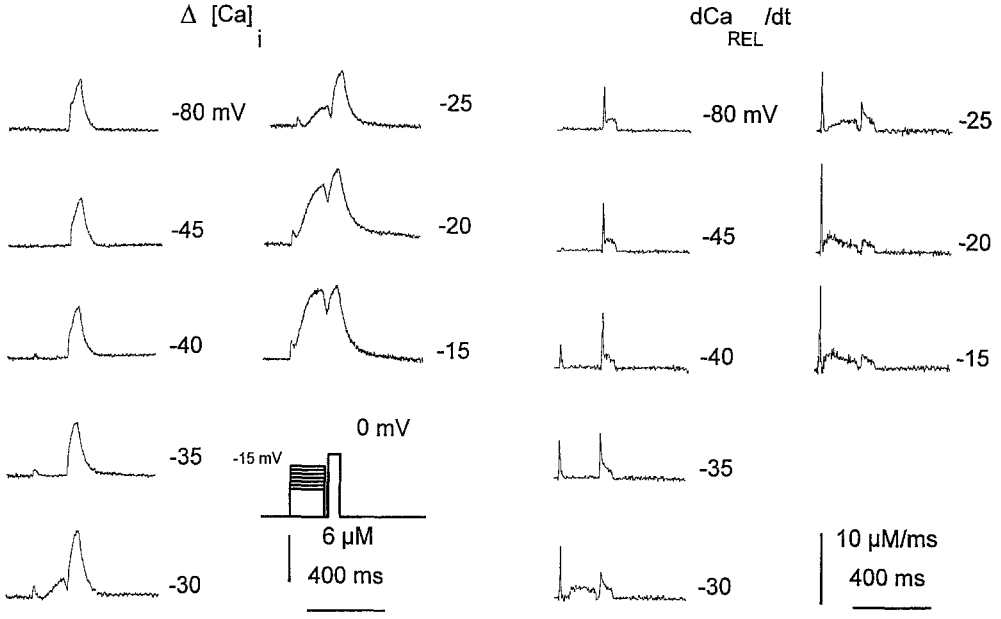

Fig. 6. The dependence of Ca^{2+} release inactivation on long prepulses at constant interpulse interval. Ca^{2+} transients ($\Delta[Ca^{2+}]_i$ measured with fura-2 and their corresponding calculated Ca^{2+} release (dCa_{REL}/dt) elicited by long pre-pulses (200 msec duration) at different potentials (pulse protocol at the bottom).

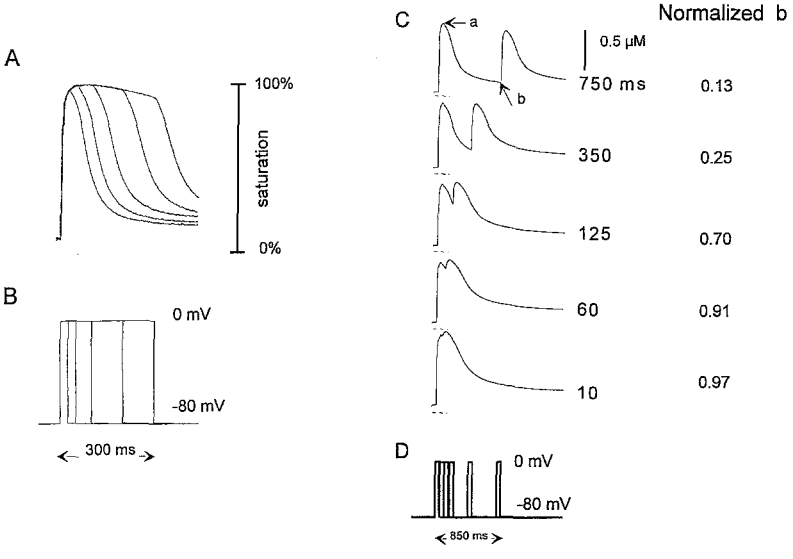

Fig. 7. $[Ca^{2+}]_i$ recorded with fura-2. (*A*) Ca^{2+} transients elicited by different pulse durations. (*B*) Pulse protocol. (*C*) Ca^{2+} transients elicited by applying a double pulse protocol (*D*). The intervals between pre- and test-pulses and normalized *b* values ($[Ca^{2+}]_i$ immediately before the test pulse), corresponding to the experiment in *C*, are shown on the right. Resting $[Ca^{2+}]_i$ before pulsing the fiber is represented as dotted lines in *C*.

Ca^{2+} Release Inactivation is not Mediated by Charge Immobilization

Charge movements were recorded simultaneously with intracellular calcium transients by blocking I_{Ca} with 2 mM Co^{2+} in the external solution. The integral of the charge movement current at the beginning of fiber depolarization (Q_{on}) and after repolarization (Q_{off}) were recorded during prepulses and test pulses. No charge immobilization was detected with variable prepulses (30 to 120 msec) at 0 mV in the test pulses. Fig. 9*A* shows charge movement records corresponding to the Ca^{2+} transients shown in Fig. 4 (250 msec interval). The Q_{on} (prepulse)/Q_{off} (test pulse) ratio was 0.98 ± 0.02 (n = 10). Fig. 9*B* shows charge movement conservation and lack of changes in voltage dependence from −80 to + 30 mV for pre- (triangles) and test pulses (circles). Experimental values were fitted to a single Boltzmann equation ($Q = Q_{max}/(1 + \exp(V_{1/2} - V/k))$), where Q_{max} is the maximum charge moved, $V_{1/2}$ is the midpoint potential of the curve, and k is the steepness of the curve. The best fit of the data gave the following values for the prepulses Q_{max}

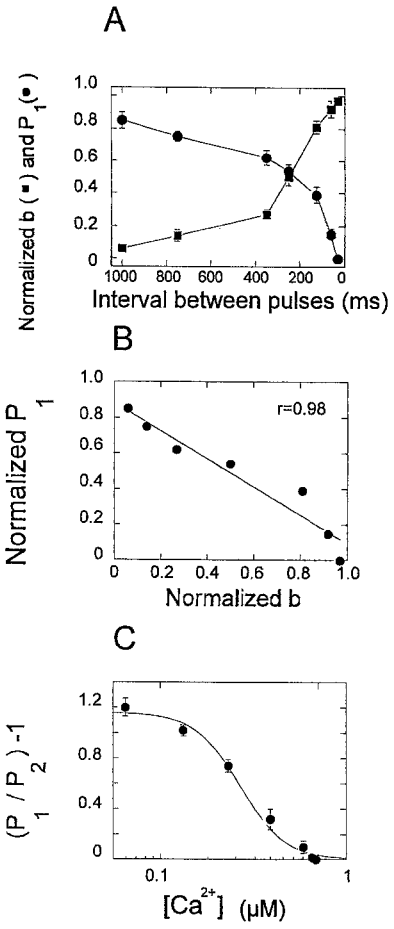

Fig. 8. Ca^{2+}-dependence of Ca^{2+} release inactivation. (*A*) Normalized *b* values and P_1 at different intervals between pulses. (*B*) Correlation between normalized P_1 and normalized *b*. (*C*) Semilog plot of the $(P_1/P_2) - 1$ *vs.* $[Ca^{2+}]_i$ relationship. The values were fitted to the equation described in the text. Values are means ± SEM.

$= 11.8\ nC/\mu F$, $V_{1/2} = -25.9$ mV and $k = 14.0$ mV. Values of the fitting for the test pulses were: $Q_{max} = 11.6\ nC/F$, $V_{q1/2} = -25.8$ mV and $k = 13.8$ mV (n = 10). As can be seen, the fitting curves are superimposed. In summary, no changes in the voltage dependence of charge movement was seen in response to test pulses. Thus, calcium effect on the voltage sensor can not account for SR calcium release inactivation.

Discussion

Ca^{2+} Regulation of Sarcoplasmic Reticulum Ca^{2+} Release

Three main processes reduce or interrupt sarcoplasmic reticulum Ca^{2+} release, inactivation of the Ca^{2+} release channel, sarcoplasmic reticulum Ca^{2+} depletion (Baylor et al., 1983, 1988; Smith et al., 1986; Schneider, Ríos &

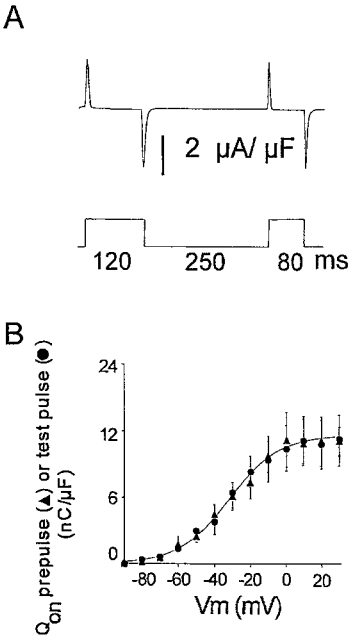

Fig. 9. Charge movements record in 2 mM Co^{2+} (*A*) Prepulse, postpulse and interval between pulses are shown on the pulse protocol. Q_{on} prepulse or test pulse—Vm relationship was fitted to a Boltzmann equation. For fitting parameters *see* text. Values are means ± SEM.

Meltzer, 1987; Schneider et al., 1987) and, Ca^{2+} release channel adaptation (Györke & Fill, 1993; Yasui, Palade & Györke, 1994; Györke & Palade, 1994; Györke, Vélez, Suárez-Isla & Fill, 1994). Sarcoplasmic reticulum Ca^{2+} depletion is not a prominent phenomenon in rat compared to frog fibers. In addition, the rate of Ca^{2+} release during prepulses were reproducible in shape and amplitude in the same fiber ruling out a progressive and slow Ca^{2+} depletion in the sarcoplasmic reticulum. Ca^{2+} release channel adaptation can account for some differences in the magnitude of the Ca^{2+} release inactivation measured in some fibers.

Two Phases of Inactivable Calcium Release

Recent publications describe some aspects of Ca^{2+} release kinetics in rat fast-twitch fibers (Delbono et al., 1993*b*; García et al., 1993). Ca^{2+} transients in rat fibers have a complex rising phase. This means that after a steep $[Ca^{2+}]$ increase, a transient plateau or a notch is recorded, then a second slower increase in myoplasmic $[Ca^{2+}]$ can be measured. In frog fibers, monophasic or biphasic activations, have been reported (Simon et al., 1988, 1991; Brum et al., 1988). In rat fibers, Ca^{2+} release shows an initial peak that rapidly inactivates, followed by a second slower and smaller phase. The same Ca^{2+} release shape has been reported using mag-fura-5 (Delbono et al., 1993*b*) and differs from that recorded in frog (Meltzer et al., 1986) and in rat, by other authors (García et al., 1993). Differences in the Ca^{2+} release

"steady state" phase can not be ascribed to intrinsic properties of the dye, since experiments in frog using mag-fura-2, showed a monoexponential Ca^{2+} flux decay (Delbono, *unpublished data*). Nonexcluding interpretations for the complex Ca^{2+} release inaction are: (i) a nonlinear removal system (Brum et al., 1988) associated with a larger calcium release, (ii) a secondary Ca^{2+} gated-Ca^{2+} release. Some experimental evidence supports a prolonged regenerative Ca^{2+} release (Ca^{2+}-gated Ca^{2+} release) throughout fiber depolarization: (a) the amplitude of the secondary Ca^{2+} release can be modulated by long or very positive depolarizations, (b) conditioning pulses may also modify the amplitude and time course of this phase and, (c) high intracellular BAPTA concentration can suppress both the first and second phases of Ca^{2+} release, remaining a component which is noninactivable by calcium (Jacquemond et al., 1991; Delbono et al., 1993*a*).

Different internal cations have been used in rat fiber experiments (Delbono et al., 1993; García et al., 1993). However, it is unlikely that this methodological variant can afford for differences in Ca^{2+} release. Another factor to be regarded is the simultaneous use of a high K_D with a low K_D Ca^{2+} indicator in other work (García et al., 1993). There is not consensus about the effect of millimolar concentrations of high affinity Ca^{2+} buffers on frog fibers calcium inactivation (Jacquemond, 1991; Jong et al., 1994). In rat fibers, BAPTA reduces the amount of Ca^{2+} release in a concentration-dependent manner (Delbono et al., 1993*a*), which may suggest that fura-2 may preclude the detection of a second Ca^{2+}-dependent positive feedback on Ca^{2+} release. In summary, it is likely that a Ca^{2+}-gated Ca^{2+} release mechanism operates throughout fiber activation, in rat EDL fibers.

The contribution from Ca^{2+} current (I_{Ca}) to the calcium release records can be overlooked in this preparation. No changes in Ca^{2+} transients and Ca^{2+} release have been recorded after blocking the Ca^{2+} conductance with mM Co^{2+}. In addition, a secondary Ca^{2+} release was recorded by applying short pulses (30 msec, Fig. 4) and/or positive potentials (+30 mV). With this pulse protocol I_{Ca} is barely activated or inactivated in rat EDL fibers (Delbono, 1992).

It has been reported that at last two RYR isoforms express in mammalian skeletal muscle (RYR1 and RYR3) with different affinities for calcium (Sorrentino et al., 1993). A complex Ca^{2+}-gated calcium release may reflect the activation/inactivation process of RYR isoforms. In support of this concept is the experimental evidence that Ca^{2+} release studied with the low K_D calcium indicator fura-2 shows an inactivating followed by a noninactivating phase (Delbono et al., 1993*b*). Probably, more RYR subpopulations, will be described, providing a structural basis for more sensitive fluorescent Ca^{2+} measurements in muscle fibers.

Model-dependent Interpretation of Ca^{2+} Regulation of Sarcoplasmic Reticulum Ca^{2+} Release

These experiments demonstrate that longer pulses induce larger residual $[Ca^{2+}]_i$, and the correlation between the peak Ca^{2+} release and b is high. These data suggest that Ca^{2+} binds and inactivates the Ca^{2+} release channel. The $[(P_1/P_2)\text{-}1]\text{-}[Ca^{2+}]$ relationship demonstrates that the number of Ca^{2+} ions bound to the Ca^{2+} release channel to induce half inactivation of the rate of Ca^{2+} release was similar to that described in rat and other species (Simon et al., 1991; García & Schneider, 1993). In rat EDL fibers, the half dCa_{REL}/dt inactivation was recorded in 0.25 μM $[Ca^{2+}]_i$. Experiments in amphibians show a similar half $[Ca^{2+}]$ inactivating value, 0.3 μM (Simon et al., 1991). These values are lower than those reported for rabbit and rat heavy SR membranes reconstituted into lipid bilayer (Meissner et al., 1986; Delbono, Stefani & Chu, 1993). One explanation for this discrepancy is that at potentials, the calcium concentration in the microenvironment of the Ca^{2+} release channel is higher than in other regions of the sarcomere space (Escobar et al., 1994).

Ca^{2+} release inactivation cannot be explained by an effect on gating currents. In this work and in frog fibers it has been demonstrated that gating currents are completely recovered and the end of the test pulses (*see* Results, Simon et al., 1991).

In summary, this work supports a direct action of Ca^{2+} on the Ca^{2+} release channel in mammalian fast-twitch skeletal muscle fibers. Mycoplasmic $[Ca^{2+}]$ inactivates the fast Ca^{2+} release and a secondary slow component. This means that in addition to the voltage-activated Ca^{2+} release, a complex calcium gating mechanism operates in rat muscle fibers.

This work was supported by Grant-in-Aid from the American Heart Association (National) and Muscular Dystrophy Association (USA). Part of this work was developed in Dr. Stefani's laboratory at Baylor College of Medicine.

References

Baylor, S.M., Chandler, W.K., Marshall, M.W. 1983. Sarcoplasmic reticulum calcium release in frog skeletal muscle estimated from arzenazo III calcium transients. *J. Physiol.* **344:**625–666

Baylor, S.M., Hollingworth, S. 1988. Fura-2 calcium transients in frog skeletal muscle fibers. *J. Physiol.* **403:**151–192

Brum, G., Rios, E., Stefani, E. 1988. Effect of extracellular calcium movements of excitation-contraction coupling in frog skeletal muscle fibers. *J. Physiol.* **398:**441–473

Csernoch, L., Jacquemond, V., Kao, J.P.Y., Schneider, M.F. 1992. The effect of BAPTA type calcium buffers on the calcium release in frog skeletal muscle fibers. *Biophys. J.* **61:**A23

Delbono, O. 1992. Calcium current activation and charge movement in denervated mammalian skeletal muscle fibers. *J. Physiol.* **451:**187–203

Delbono, O., Stefani, E. 1993*a*. Ca^{2+} modulation of SR Ca^{2+} release in mammalian skeletal muscle fibers. *Biophys. J.* **61:**A160

Delbono, O., Stefani, E. 1993*b*. Calcium transients in single mammalian skeletal muscle fibers. *J. Physiol.* **463:**689–707

Delbono, O., García, J., Appel, S.H., Stefani, E. 1991. Kinetics of the dihydropyridine sensitive calcium current (I_{Ca}) of mammalian skeletal muscle fibers: action of ALS IgG. *J. Physiol.* **444,** 723–742

Delbono, O., Stefani, E., Chu, A. 1993. Characterization of Ca release channels from denervated rats. *Biophys. J.* **64:**A151

Escobar, A.L., Monck, J.R., Fernandez, J.M., Vergara, J.L. 1994. Localization of the site of Ca^{2+} release at the level of a single sarcomere in skeletal muscle fibres. *Nature* **367:**739–741

Fabiato, A. 1988. Computer programs for calculating total from specified free or free from specified total ionic concentrations in aqueous solutions containing multiple metals and ligands. *In:* Methods in Enzymology, Biomembranes. S. Fleisher and B. Fleisher, editors. p. 378–417. **157** (Part A)

Francini, F., Stefani, E. 1989. Decay of the slow calcium current in twitch muscle fibers of the frog is influenced by intracellular EGTA. *J. Gen. Physiol* **94:**953–969

García, J., Schneider, M.F. 1993. Calcium transients and calcium release in rat fast-twitch skeletal muscle fibres. *J. Physiol.* **463:**709–728

González, A., Ríos, E. 1993. Perchlorate enhances transmission in skeletal muscle excitation-contraction coupling. *J. Gen. Physiol.* **102:**373–421

Györke, S., Fill, M. 1993. Ryanodine receptor adaptation: control mechanism of Ca^{2+}-induced Ca^{2+} release in heart. *Science* **260:**807–809

Györke, S., Palade, P. 1994. Ca^{2+}-dependent negative control mechanism for Ca^{2+}-induced Ca^{2+} release in crayfish muscle. *J. Physiol.* **476:**315–322

Györke, S., Vélez, P., Suárez-Isla, B., Fill, M. 1993. Activation of single cardiac and skeletal ryanodine receptor channels by flash photolysis of caged Ca^{2+}. *Biophys. J.* **66:**1879–1886

Herrmann-Frank, A., Varsányi, M. 1993. Enhancement of Ca^{2+} release channel activity by phosphorylation of the skeletal muscle ryanodine receptor. *FEBS Let.* **332:**237–242

Jacquemond, V., Csernoch, L., Klein, M.G., Schneider, M.F. 1991. Voltage-gated and calcium-gated calcium release during depolarization of skeletal muscle fibers. *Biophys. J.* **60:**867–873

Jong, D.S., Pape, P.C., Chandler, W.K., Baylor, S.M. 1993. Reduction of calcium inactivation of sarcoplasmic reticulum calcium release by fura-2 in voltage-clamped cut twitch fibers from frog muscle. *J. Gen. Physiol.* **102:**333–370

Konishi, M., Hollingworth, S., Harkins, A.B., Baylor, S.M. 1991. Myoplasmic calcium transients in intact frog skeletal muscle fibers monitored with the fluorescent indicator furaptra. *J. Gen. Physiol.* **97:**271–301

Meissner, G., Darling, E., Eveleth, J. 1986. Kinetics of rapid Ca^{2+} release by sarcoplasmic reticulum: effects of Ca^{2+}, Mg^{2+}, and adenine nucleotides. *Biochem.* **25:**236–244

Melzer, W., Rios, E., Schneider, M.F. 1986. The removal of myoplasmic free calcium following calcium release in frog skeletal muscle. *J. Physiol.* **373:**261–292

Melzer, W., Rios, E., Schneider, M.F. 1987. A general procedure for determining the rate of calcium release from the sarcoplasmic reticulum in skeletal muscle fibers. *Biophys. J.* **51:**849–863

O'Brien, J., Meissner, G., Block, B.A. 1993. The fastest contracting muscles of nonmammalian vertebrates express only one isoform of the ryanodine receptor. *Biophys. J.* **65:**2418–2427

Olivares, E.B., Tanksley, S.J., Airey, J.A., Beck, C., Ouyang, Y., Deerinck, T.J., Ellisman, M.H., Sutko, J.L. 1991. Nonmammalian vertebrate skeletal muscles express two triad junctional foot protein isoforms. *Biophys. J.* **59:**1153–1163

Raju, B., Murphy, E., Levy, L.A., Hall, R.D., London, R.E. 1989. A fluorescent indicator for measuring cytosolic free magnesium. *Am. J. Physiol.* **256:**C540–C548

Schneider, M.F., Simon, B.J., Szucs, G. 1987. Depletion of calcium from the sarcoplasmic reticulum during calcium release in frog skeletal muscle. *J. Physiol.* **392:**167–192

Simon, B.J., Klein, M.G., Schneider, M.F. 1991. Calcium dependence of inactivation of calcium release from the sarcoplasmic reticulum in skeletal muscle fibers. *J. Gen. Physiol.* **97:**437–471

Simon, B.J., Schneider, M.F. 1988. Time course of activation of calcium release from sarcoplasmic reticulum in skeletal muscle. *Biophys. J.* **54:**1159–1163

Smith, J.S., Coronado, R., Meissner, G. 1986. Single channel measurements of the calcium release channel from skeletal muscle sarcoplasmic reticulum. *J. Gen. Physiol.* **88:**573–588

Sorrentino, V., Volpe, P. 1993. Ryanodine receptors: how many, where and why? *TIPS* **14:**98–103

Tsien, R., Pozzan, T. 1989. Measurement of cytosolic free Ca^{2+} with Quin-2. *In:* Methods in Enzymology, Vol. 172, part S, S. Fleischer and B. Fleischer, pp. 230–262. Academic press, San Diego, CA

Yasui, K., Palade, P., Györke, S. 1994. Negative control mechanism with features of adaptation controls Ca^{2+} release in cardiac myocytes. *Biophys. J.* **67,** 457–460

Wang, J., Best, P.M. 1992. Inactivation of the sarcoplasmic reticulum calcium channel by protein kinase. *Nature* **359:**739–741